CONDENSED MATTER PHYSICS

Determination of layer-dependent exciton binding energies in few-layer black phosphorus

Guowei Zhang,[1,2] Andrey Chaves,[3] Shenyang Huang,[1,2] Fanjie Wang,[1,2] Qiaoxia Xing,[1,2] Tony Low,[4] Hugen Yan[1,2]*

Copyright © 2018 The Authors, some rights reserved; exclusive licensee American Association for the Advancement of Science. No claim to original U.S. Government Works. Distributed under a Creative Commons Attribution NonCommercial License 4.0 (CC BY-NC).

The attraction between electrons and holes in semiconductors forms excitons, which largely determine the optical properties of the hosting material, and hence the device performance, especially for low-dimensional systems. Mono- and few-layer black phosphorus (BP) are emerging two-dimensional (2D) semiconductors. Despite its fundamental importance and technological interest, experimental investigation of exciton physics has been rather limited. We report the first systematic measurement of exciton binding energies in ultrahigh-quality few-layer BP by infrared absorption spectroscopy, with layer (L) thickness ranging from 2 to 6 layers. Our experiments allow us to determine the exciton binding energy, decreasing from 213 meV (2L) to 106 meV (6L). The scaling behavior with layer numbers can be well described by an analytical model, which takes into account the nonlocal screening effect. Extrapolation to free-standing monolayer yields a large binding energy of ~800 meV. Our study provides insights into 2D excitons and their crossover from 2D to 3D, and demonstrates that few-layer BP is a promising high-quality optoelectronic material for potential infrared applications.

INTRODUCTION

Due to strong spatial confinement and reduced dielectric screening, excitons in atomically thin semiconductors are typically robust, showing binding energy one order of magnitude larger than their bulk counterpart. Moreover, the exciton energy spectrum deviates strongly from the two-dimensional (2D) hydrogen model (*1*–*3*). The question of dimensionality crossover for excitonic effects as the thickness of 2D semiconductor increases is of fundamental interest and importance. However, attempts to study the dimensionality crossover for excitonic effects in 2D transition metal dichalcogenides (TMDCs), such as MoS_2, WS_2, $MoSe_2$, and WSe_2, is inherently challenging because the bandgap is only direct for monolayers (*4*). Mono- and few-layer black phosphorus (BP) are emerging 2D direct-gap semiconductors (*5*–*8*), with the gap size strongly depending on the layer thickness (*9*–*12*). Therefore, BP provides us an ideal platform to interrogate 2D excitons and the crossover to 3D. Moreover, the anisotropy of 2D BP opens an avenue for investigation of anisotropic 2D excitons (*13*, *14*), which are expected to show exotic sequences of excited energy levels. Although these unique features of excitons in few-layer BP are of great importance for both fundamental research and device applications, the exciton binding energy is still far from conclusive. For monolayer BP on SiO_2, the exciton binding energy was first experimentally reported to be as large as 0.9 eV (*15*); however, a more recent experiment indicates that the value is only 0.1 eV for monolayer BP covered by boron nitride (*10*). Moreover, the exciton binding energies in few-layer BP are not fully determined experimentally, although valuable information has been obtained from previous measurements by Li *et al.* (*10*).

Here, we investigate the excitonic effects in few-layer BP on polydimethylsiloxane (PDMS) substrates with layer (L) number $N = 2$ to 6, using infrared (IR) absorption spectroscopy (see Materials and Methods). We find that excitonic resonances dominate the optical absorption. For the high-quality BP samples studied here, the optical absorption spectrum exhibits surprisingly sharp and intense features, with an unprecedented linewidth of <25 meV at room temperature for the band edge excitons. This high optical quality was previously unattainable because of the degradation of few-layer BP under ambient conditions (*16*). Most strikingly, the spectral features of lowest-energy excited states are clearly observable even at room temperature. In conjunction with numerical calculations, exciton binding energies are determined for 2L to 6L BP, and the binding energy for monolayer BP is also inferred. The scaling behavior of the binding energy with layer number is carefully examined. Our results pave the way for BP applications in IR optoelectronics, such as photodetection (*17*–*19*), optical modulation (*20*), lasing (*21*, *22*), and polariton condensation (*23*).

RESULTS

Exciton-dominated optical absorption

In 2D semiconductors, the optical absorption is characteristic of step-like features in the single-particle picture (*24*, *25*), with the onset of band-to-band transitions as the quasi-particle bandgap E_g. Electron-hole (e-h) interactions are found to dramatically modify the optical response, leading to new spectral features below E_g. Figure 1B illustrates the optical absorption in a model 2D semiconductor, including transitions to exciton bound states and free carrier states (continuum), with the exciton binding energy defined as $E_b = E_g - E_{opt}$, where E_{opt} is the optical gap, related to the optical transition energy of the ground state exciton.

Few-layer BP samples were directly exfoliated on PDMS substrates from bulk crystals (HQ Graphene Inc.) with areas typically over 1500 μm^2, large enough for us to obtain accurate IR extinction $(1 - T/T_0)$ spectrum, where T and T_0 denotes the light transmittance of samples on PDMS and bare PDMS, respectively. For atomically thin layers supported by a thick transparent substrate, when the optical conductivity is not large, the extinction $(1 - T/T_0)$ is approximately proportional to the real part of the optical conductivity (*26*). The layer number of BP flakes is determined by IR characterization (*9*). To obtain high optical quality of BP samples, we performed IR measurements right after the exfoliation using a Fourier

[1]Department of Physics, State Key Laboratory of Surface Physics and Key Laboratory of Micro and Nano Photonic Structures (Ministry of Education), Fudan University, Shanghai 200433, China. [2]Collaborative Innovation Center of Advanced Microstructures, Nanjing 210093, China. [3]Departamento de Física, Universidade Federal do Ceará, Caixa Postal 6030, Campus do Pici, 60455-900 Fortaleza, Ceará, Brazil. [4]Department of Electrical and Computer Engineering, University of Minnesota, Minneapolis, MN 55455, USA.
*Corresponding author. Email: hgyan@fudan.edu.cn

Downloaded from http://advances.sciencemag.org/ on November 19, 2018

transform IR (FTIR) spectrometer in combination with an IR microscope under ambient conditions. The exposure time in air with low humidity is typically <5 min. Comparative studies for samples without exposure to air have been performed. We found that such short time exposure (<5 min) to low-humidity air has little effect on the optical quality. In our previous studies (*9*), BP layers were first exfoliated on PDMS and then transferred to other substrates. The quality of such samples was typically much lower.

A representative IR extinction spectrum of a 4L BP sample on PDMS is shown in Fig. 1C, with normal light incidence and polarization along the two characteristic directions (more data for 4L BP are presented in fig. S1). In few-layer BP, conduction and valence bands split into quantized subbands because of quantum confinement in the out-of-plane direction, similar to the traditional quantum wells (QWs). Optical transitions with subband index difference $\Delta n = 0$ for valence and conduction bands are allowed in symmetric QWs (*27*, *28*). We use the symbol E_{nn} to denote the optical transition $v_n \rightarrow c_n$ at the Γ point of the 2D Brillouin zone, illustrated in Fig. 2H. Strikingly, we observed a very sharp peak (labeled as E_{11}) in the extinction spectrum for armchair (AC) light polarization, with a linewidth as narrow as ~20 meV at room temperature. The E_{11} peak has a Lorentzian line shape, characteristic of exciton absorption (*2*, *3*, *29*). This is the ground state exciton transition. For clarity, we label the ground and excited states of excitons in analogy to hydrogenic Rydberg series as 1s, 2s, etc. The extinction at the E_{11} resonance reaches ~12%, suggesting very strong light-matter interactions in these atomically thin BP layers. In addition to the 1s peak, a weak and broad peak can be clearly resolved on the high energy side, which we attribute to the 2s transition. Moreover, we can observe a relatively flat "plateau" above ~0.8 eV; this feature is attributed to the continuum band-to-band transitions (*30*, *31*). It should be noted that the narrow spectral linewidth of the 1s state is key to clearly identifying a 2s state in the absorption spectrum; otherwise, they will be merged. For zigzag (ZZ) light polarization, the spectrum is featureless as expected, with a slightly tilted nonresonant background. Because of the low symmetry of the crystal structure, the excitonic response of BP is strongly polarization-dependent (see fig. S2) (*9*, *10*, *12*, *15*).

To probe the layer dependence of excitonic response, we performed IR absorption measurements on few-layer BP from 2L to 6L, as shown in Fig. 2 (A to E). The band edge optical transitions in all samples exhibit very narrow spectral features, indicating very high sample quality. The E_{11} resonances are all spectrally sharp and intense. The 2s features can be clearly identified in the IR spectra as indicated by red arrows. Thus, the 1s-2s separation (Δ_{12}) can be directly extracted, and the values are 122, 87, 76, 62, and 58 meV for 2L to 6L samples, respectively. As previously demonstrated (*9*, *10*), the optical transition energies exhibit remarkable layer dependence because of the strong interlayer interaction (*32*). For comparison, we also performed similar IR measurements for thicker samples (7L and 8L), as shown in Fig. 2 (F and G). The 1s peaks are as sharp, but the 2s exciton features are unresolvable, presumably due to a smaller 1s-2s energy separation. Moreover, for E_{22} transitions, the exciton peak is broader, indicating a shorter exciton lifetime for higher energy transitions. This is reasonable because carriers at the higher subband would energetically relax toward the band edges. Nevertheless, the E_{22} peaks are still very clear, in sharp contrast to the featureless band-to-band continuum transitions, a manifestation of exciton transitions as well.

Extraction of the exciton binding energy

In a 2D hydrogen model, it is well known that the 1s-2s separation accounts for eight-ninths of the total exciton binding energy. With the measured 1s and 2s transition energies, the exciton binding energy would then become $E_b = 9/8\Delta_{12}$. However, this picture was found to break down in atomically thin 2D crystals, such as TMDC monolayers, because of the nonlocal dielectric screening of Coulomb interactions (*1*–*3*). In 2D case, both the material itself and its surroundings contribute to the dielectric screening. Generally, the dielectric constant of the material is far greater than that of its surroundings. For higher-order excited excitonic states, the e-h spatial separation is larger, so the electric

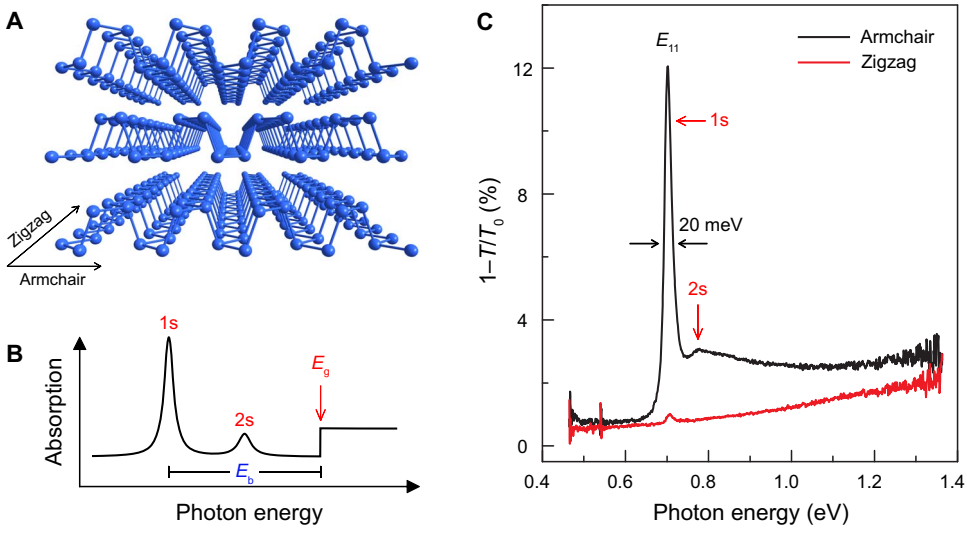

Fig. 1. Optical absorption in 2D semiconductors. (**A**) Lattice structure of few-layer BP, showing the puckered hexagonal crystal with two characteristic directions: AC and ZZ. (**B**) Illustration of optical absorption in a model conventional 2D semiconductor, including optical transitions to excitonic ground (1s) and excited states (2s), as well as continuum states above the quasi-particle bandgap E_g. The exciton resonance is characteristic of a Lorentzian line shape, whereas the continuum absorption exhibits a step-like feature. (**C**) IR extinction spectra ($1 - T/T_0$) for a representative 4L BP sample on a PDMS substrate, with two different light polarizations. The symbol E_{11} denotes exciton relating to optical transition $v_1 \rightarrow c_1$, as illustrated in Fig. 2H. Data were collected at room temperature.

Downloaded from http://advances.sciencemag.org/ on November 19, 2018

field lines would experience a larger portion of screening from the surroundings. Consequently, the effective screening is significantly reduced, and this effect is also known as the anti-screening effect (*1*). The nonuniform dielectric environments result in a pronounced deviation of the excitonic states from the 2D hydrogenic Rydberg series, and the simple relation $E_b = 9/8\Delta_{12}$ does not hold. Nevertheless, the observed 2s features in our experiments are still very informative, because the energy separation from the 1s transition can give us a lower bound of the exciton binding energy. In fact, in combination with numerical calculation, we are able to determine the exciton binding energies, and hence the quasi-particle bandgaps.

To extract the exciton binding energy, we calculate the excitonic states in few-layer BP on PDMS substrates (N = 2 to 6) within the Wannier-Mott framework (see the Supplementary Materials for details) by solving the Schrödinger equation numerically (*14*, *33*). As shown in Fig. 3A, the calculated 1s-2s separation agrees very well with our experimental observations, confirming the assignment of the weak features to 2s transitions. Furthermore, the exciton binding energies are extracted to be 213, 167, 139, 120, and 106 meV, respectively. Even larger values are expected for suspended samples, because generally E_b is inversely proportional to ε^2 (ε is the dielectric constant) and the screening from the underlying substrate is expected to significantly reduce the exciton binding energy. This large binding energy in few-layer BP is one order of magnitude larger than that in bulk BP (*34*), mainly originating from the weak dielectric screening and strong quantum confinement in 2D case. The binding energies determined here are in good agreement with previous theoretical calculations (*14*, *35*).

One may notice that the 1s-2s separation only accounts for about half of the total exciton binding energy, rather than eight-ninths predicted in the 2D hydrogen model, that is, the observed exciton series in few-layer BP is nonhydrogenic, a very general feature in 2D semiconductors (*3*). In addition, the exciton binding energy decreases with increasing layer number, showing strong thickness dependence. Relative to the 1s transition energy (optical gap), we extracted the quasi-particle bandgap for 2L to 6L BP as $E_g = E_{opt} + E_b$, and the values are 1.33, 1.01, 0.84, 0.73, and 0.66 eV, respectively, summarized in Fig. 3B, exhibiting strong layer dependence as predicted by previous calculations (*11*, *12*).

Layer dependence of the exciton binding energy

The layer dependence of the exciton binding energy is of particular interest, given that it can shed light on the dimensional crossover from 2D to 3D for excitons. Recently, Olsen *et al.* (*36*) proposed a simple screened hydrogen model to describe excitons in 2D materials. E_b has an analytical expression as a function of the reduced effective mass μ of excitons and the sheet polarizability α:

$$E_b = \frac{2\mu}{(m-1/2)^2\left(1+\sqrt{1+\frac{32\pi\alpha\mu}{9m(m-1)+3}}\right)^2}$$, where m is the s-state index and the equation is in atomic units. Under the condition $32\pi\mu\alpha/3 >> 1$, E_b for ground state exciton (m = 1) can be simplified as $E_b \approx \frac{3}{4\pi\alpha}$, which is proved to be valid over a wide range of 2D TMDCs (*36*) and should also work for few-layer BP. This indicates that the exciton binding energy of 2D materials is solely determined by its polarizability and does not directly depend on the effective mass, in sharp contrast to the 3D case. The 2D polarizability relates to the screening effect and can be viewed as the in-plane component of the 3D polarizability in its bulk counterparts. The effect of the substrate can also be included, by simply

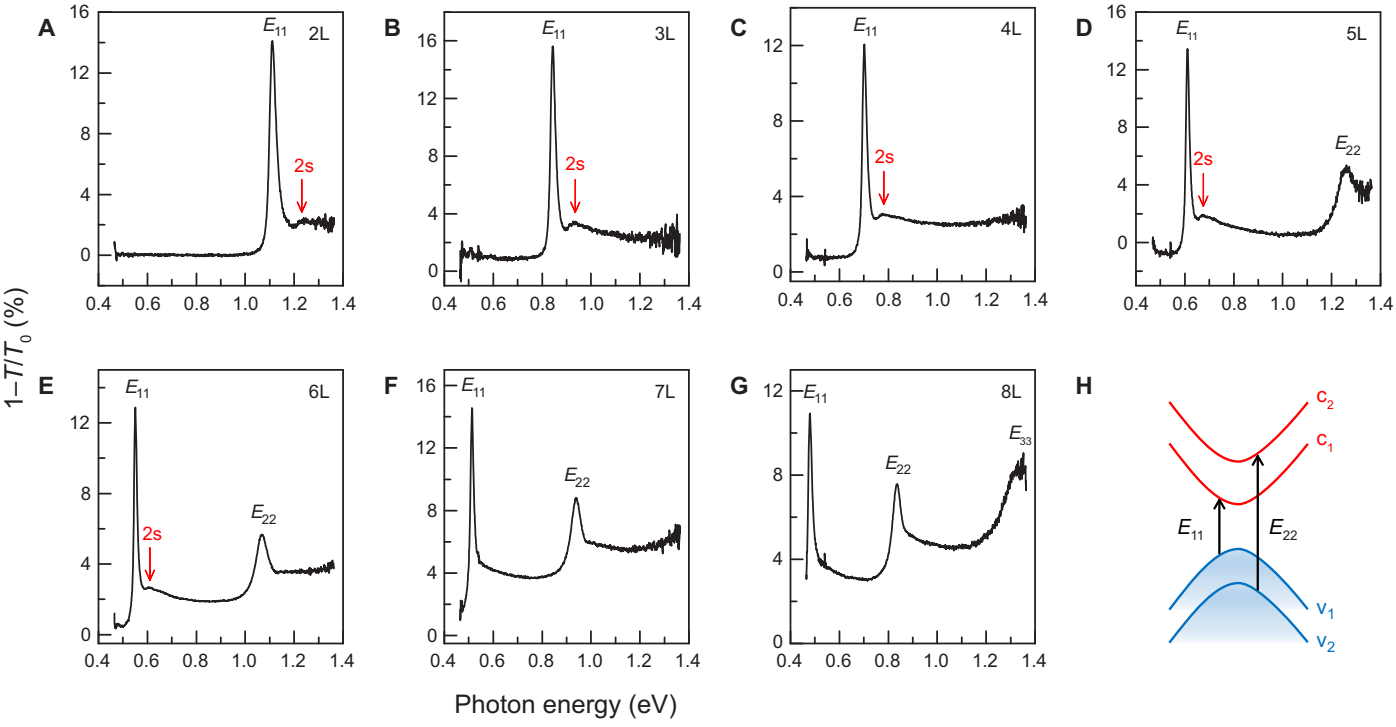

Fig. 2. Layer-dependent IR extinction spectra. (**A** to **G**) IR extinction spectra ($1 - T/T_0$) for few-layer BP on PDMS substrates with layer number N = 2 to 8, with incident light polarized along the AC direction. The red arrows indicate the lowest-energy excited states (2s) of the E_{11} transition. For 7L and 8L samples, the 2s peaks are unresolvable. (**H**) Schematic illustration of optical transitions between quantized subbands in few-layer BP, with the symbols E_{11} and E_{22} denoting transitions $v_1 \rightarrow c_1$ and $v_2 \rightarrow c_2$, respectively.

Downloaded from http://advances.sciencemag.org/ on November 19, 2018

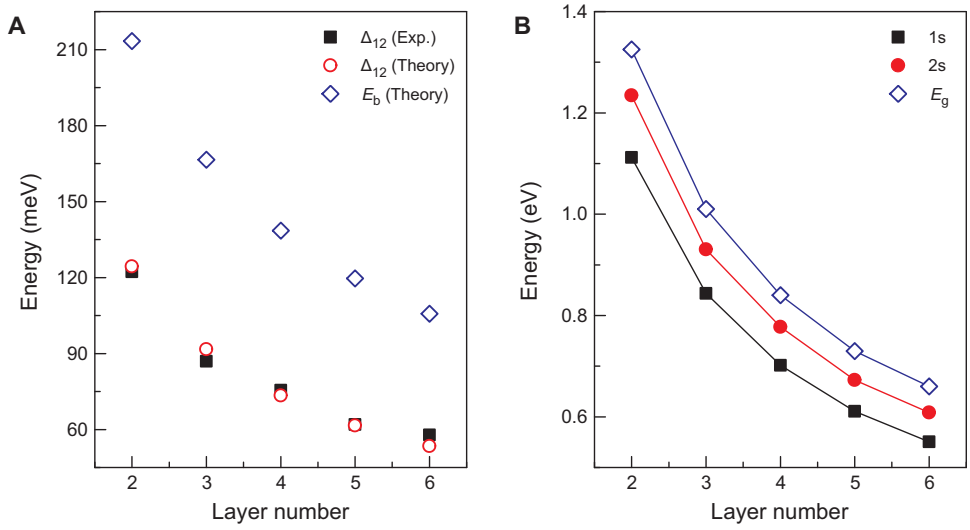

Fig. 3. Extraction of the exciton binding energies and quasi-particle bandgaps. (**A**) Experimentally and theoretically obtained 1s-2s separation (Δ_{12}) as a function of layer number. The blue diamonds denote the exciton binding energy obtained using a numerical method detailed in the Supplementary Materials. (**B**) Layer dependence of the 1s and 2s transition energies and the quasi-particle bandgap. The 1s and 2s transition energies are obtained experimentally, as indicated in Fig. 2. The quasi-particle bandgap is deduced as $E_g = E_{opt} + E_b$, where E_{opt} is the 1s transition energy.

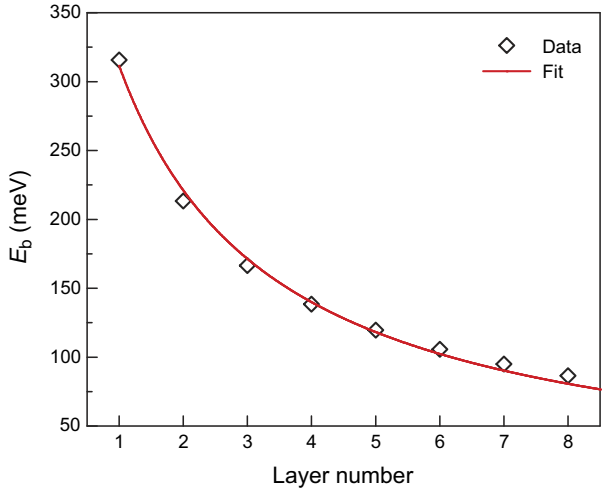

Fig. 4. Scaling behavior of the exciton binding energy with layer number. The black diamonds are theoretical values for few-layer BP with N = 1 to 8 obtained within the Wannier-Mott framework. The red line is a fit to the data, using the formula $E_b = 3/4\pi\alpha_{eff}$. α_{eff} is the effective 2D polarizability, with a linear function of layer number N: $\alpha_{eff} = \alpha_0 + N\alpha_1$, where α_0 and $N\alpha_1$ describe the screening effect from the underlying substrate and the 2D material itself, respectively.

replacing the polarizability α with an effective value α_{eff}. This effective polarizability should also depend on the substrate, in addition to the polarizability of the 2D material. For a few-layer BP, we can still treat it as a 2D system in the limit where the thickness is small compared to the exciton Bohr radius. Simple estimation based on the effective masses and dielectric constant of bulk BP gives a Bohr radius of ~5 nm (*12*, *37*), which validates the approximation in our case. Because the polarizability of BP is approximately equal to its density of states (*38*), it scales roughly with the layer number. Hence, we propose a layer-dependent effective sheet polarizability $\alpha_{eff}(N) = \alpha_0 + N\alpha_1$, where α_0 and $N\alpha_1$ account for the screening from the underlying substrate and the 2D material itself, respectively. With this linear relation between α_{eff} and N, we have (in atomic units)

$$E_b = \frac{3}{4\pi(\alpha_0 + N\alpha_1)} \quad (1)$$

Figure 4 plots numerically obtained E_b as a function of N. In addition to the data points shown in Fig. 3, more data points for 1L, 7L, and 8L samples are also shown here, obtained using the same numerical methods (see the Supplementary Materials). We use Eq. 1 to fit our data. With fitting parameters α_0 = 6.5 Å and α_1 = 4.5 Å, it shows excellent agreement. The value for α_1 extracted here matches well with previous calculations (α_1 = 4.1 Å) (*13*). These parameters are very reasonable given that the bulk dielectric constant ε for BP is ~10ε_0 (*37*). Compared to the 3D counterparts, two main factors determine the exciton binding energies for a 2D material, namely, the reduced screening and spatial confinement in the out-of-plane direction. When increasing the layer number, Eq. 1 does not take into account the reduced confinement and only the screening increase is considered. The good agreement with data shows that in the small thickness limit, the screening effect plays a dominant role. Of course, the model breaks down when the thickness is much larger than the Bohr radius and a 3D-type exciton model will be required to further describe the crossover from 2D to 3D.

With the fitting parameter α_1 = 4.5 Å and by setting α_0 = 0, we can infer the binding energies for free-standing few-layer BP: E_b = 762/N meV, as shown in fig. S3. The free-standing monolayer BP has an exciton binding energy of 762 meV, in good agreement with ab initio calculations based on the Bethe-Saltpeter equation framework, which gives E_b ~ 800 meV (*12*). E_b for monolayer BP on PDMS is 316 meV, less than half of that for free-standing samples, indicating the importance of the substrate screening effect. Our systematic study does not agree with the previous study of excitons in monolayer BP on SiO_2 (*15*), which claims a much larger E_b of 900 meV, despite similar

Downloaded from http://advances.sciencemag.org/ on November 19, 2018

dielectric constants of SiO_2 and PDMS. Certainly, further experiments would help in resolving this discrepancy.

DISCUSSION

In summary, with ultrahigh optical quality samples, we successfully determined the exciton binding energies for 2L to 6L BP. The large binding energy we observed here shows strong layer dependence, in good agreement with a model that solely takes into account the linear increase of the sheet polarizability in the quasi-2D limit. This sheds light on the exciton crossover from 2D to 3D. The strong excitonic effects are expected to profoundly affect the device performance in BP optoelectronics even at room temperature. Few-layer BP provides us an ideal 2D system to study the layer-dependent many-body physics, such as excitons and trions (charged excitons). Moreover, as a high optical quality anisotropic 2D system, few-layer BP opens an avenue to study anisotropic 2D excitons (*13*, *14*), where light polarization can be leveraged to selectively excite excitons with different angular momenta. The ultrahigh sample quality facilitates us to probe the dark excitonic states in few-layer BP using two-photon photoluminescence excitation spectroscopy (*2*, *3*, *29*).

MATERIALS AND METHODS

Polarized IR absorption spectroscopy

The polarization-resolved IR measurements on few-layer BP were performed using a Bruker FTIR spectrometer (Vertex 70v) equipped with a Hyperion 2000 microscope. A tungsten halogen lamp was used as the light source to cover the broad spectral range 3750 to 11000 cm^{-1} (0.36 to 1.36 eV), in combination with a liquid nitrogen–cooled mercury-cadmium-telluride detector. The lower bound cutoff photon energy was restricted by the PDMS substrate. The incident light was focused on BP flakes using a 15× IR objective, with the polarization controlled by a broadband ZnSe grid polarizer. All the measurements were conducted at room temperature under ambient conditions with low humidity (<30%).

SUPPLEMENTARY MATERIALS

Supplementary material for this article is available at http://advances.sciencemag.org/cgi/content/full/4/3/eaap9977/DC1

note S1. Anisotropic optical absorption
note S2. Numerical calculation of the exciton binding energy
note S3. Substrate screening effect on the exciton binding energy
fig. S1. Additional IR extinction data for 4L and 6L BP.
fig. S2. Polarized IR extinction spectra for an 8L BP.
fig. S3. Comparison of exciton binding energies for suspended and supported few-layer BP.
table S1. Summary of experimentally and theoretically obtained values for 1s-2s separation (Δ_{12}), as well as the exciton binding energy (E_b).
References (*39*–*43*)

REFERENCES AND NOTES

1. A. Chernikov, T. C. Berkelbach, H. M. Hill, A. Rigosi, Y. Li, O. B. Aslan, D. R. Reichman, M. S. Hybertsen, T. F. Heinz, Exciton binding energy and nonhydrogenic Rydberg series in monolayer WS_2. *Phys. Rev. Lett.* **113**, 076802 (2014).
2. K. He, N. Kumar, L. Zhao, Z. Wang, K. F. Mak, H. Zhao, J. Shan, Tightly bound excitons in monolayer WSe_2. *Phys. Rev. Lett.* **113**, 026803 (2014).
3. Z. Ye, T. Cao, K. O'Brien, H. Zhu, X. Yin, Y. Wang, S. G. Louie, X. Zhang, Probing excitonic dark states in single-layer tungsten disulphide. *Nature* **513**, 214–218 (2014).
4. K. F. Mak, C. Lee, J. Hone, J. Shan, T. F. Heinz, Atomically thin MoS_2: A new direct-gap semiconductor. *Phys. Rev. Lett.* **105**, 136805 (2010).
5. L. Li, Y. Yu, G. J. Ye, Q. Ge, X. Ou, H. Wu, D. Feng, X. H. Chen, Y. Zhang, Black phosphorus field-effect transistors. *Nat. Nanotechnol.* **9**, 372–377 (2014).
6. H. Liu, A. T. Neal, Z. Zhu, Z. Luo, X. Xu, D. Tománek, P. D. Ye, Phosphorene: An unexplored 2D semiconductor with a high hole mobility. *ACS Nano* **8**, 4033–4041 (2014).
7. F. Xia, H. Wang, Y. Jia, Rediscovering black phosphorus as an anisotropic layered material for optoelectronics and electronics. *Nat. Commun.* **5**, 4458 (2014).
8. S. P. Koenig, R. A. Doganov, H. Schmidt, A. H. Castro Neto, B. Özyilmaz, Electric field effect in ultrathin black phosphorus. *Appl. Phys. Lett.* **104**, 103106 (2014).
9. G. Zhang, S. Huang, A. Chaves, C. Song, V. O. Özçelik, T. Low, H. Yan, Infrared fingerprints of few-layer black phosphorus. *Nat. Commun.* **8**, 14071 (2017).
10. L. Li, J. Kim, C. Jin, G. J. Ye, D. Y. Qiu, F. H. da Jornada, Z. Shi, L. Chen, Z. Zhang, F. Yang, K. Watanabe, T. Taniguchi, W. Ren, S. G. Louie, X. H. Chen, Y. Zhang, F. Wang, Direct observation of the layer-dependent electronic structure in phosphorene. *Nat. Nanotechnol.* **12**, 21–25 (2017).
11. J. Qiao, X. Kong, Z.-X. Hu, F. Yang, W. Ji, High-mobility transport anisotropy and linear dichroism in few-layer black phosphorus. *Nat. Commun.* **5**, 4475 (2014).
12. V. Tran, R. Soklaski, Y. Liang, L. Yang, Layer-controlled band gap and anisotropic excitons in few-layer black phosphorus. *Phys. Rev. B* **89**, 235319 (2014).
13. A. S. Rodin, A. Carvalho, A. H. Castro Neto, Excitons in anisotropic two-dimensional semiconducting crystals. *Phys. Rev. B* **90**, 075429 (2014).
14. A. Chaves, T. Low, P. Avouris, D. Çakır, F. M. Peeters, Anisotropic exciton Stark shift in black phosphorus. *Phys. Rev. B* **91**, 155311 (2015).
15. X. Wang, A. M. Jones, K. L. Seyler, V. Tran, Y. Jia, H. Zhao, H. Wang, L. Yang, X. Xu, F. Xia, Highly anisotropic and robust excitons in monolayer black phosphorus. *Nat. Nanotechnol.* **10**, 517–521 (2015).
16. A. Favron, E. Gaufrès, F. Fossard, A.-L. Phaneuf-L'Heureux, N. Y.-W. Tang, P. L. Lévesque, A. Loiseau, R. Leonelli, S. Francoeur, R. Martel, Photooxidation and quantum confinement effects in exfoliated black phosphorus. *Nat. Mater.* **14**, 826–832 (2015).
17. Q. Guo, A. Pospischil, M. Bhuiyan, H. Jiang, H. Tian, D. Farmer, B. Deng, C. Li, S.-J. Han, H. Wang, Q. Xia, T.-P. Ma, T. Mueller, F. Xia, Black phosphorus mid-infrared photodetectors with high gain. *Nano Lett.* **16**, 4648–4655 (2016).
18. N. Youngblood, C. Chen, S. J. Koester, M. Li, Waveguide-integrated black phosphorus photodetector with high responsivity and low dark current. *Nat. Photon.* **9**, 247–252 (2015).
19. H. Yuan, X. Liu, F. Afshinmanesh, W. Li, G. Xu, J. Sun, B. Lian, A. G. Curto, G. Ye, Y. Hikita, Z. Shen, S.-C. Zhang, X. Chen, M. Brongersma, H. Y. Hwang, Y. Cui, Polarization-sensitive broadband photodetector using a black phosphorus vertical p-n junction. *Nat. Nanotechnol.* **10**, 707–713 (2015).
20. D. A. B. Miller, D. S. Chemla, T. C. Damen, A. C. Gossard, W. Wiegmann, T. H. Wood, C. A. Burrus, Band-edge electroabsorption in quantum well structures: The quantum-confined Stark effect. *Phys. Rev. Lett.* **53**, 2173–2176 (1984).
21. Y. Ye, Z. J. Wong, X. Lu, X. Ni, H. Zhu, X. Chen, Y. Wang, X. Zhang, Monolayer excitonic laser. *Nat. Photon.* **9**, 733–737 (2015).
22. S. Wu, S. Buckley, J. R. Schaibley, L. Feng, J. Yan, D. G. Mandrus, F. Hatami, W. Yao, J. Vučković, A. Majumdar, X. Xu, Monolayer semiconductor nanocavity lasers with ultralow thresholds. *Nature* **520**, 69–72 (2015).
23. T. Byrnes, N. Y. Kim, Y. Yamamoto, Exciton–polariton condensates. *Nat. Phys.* **10**, 803–813 (2014).
24. M. M. Ugeda, A. J. Bradley, S.-F. Shi, F. H. da Jornada, Y. Zhang, D. Y. Qiu, W. Ruan, S.-K. Mo, Z. Hussain, Z.-X. Shen, F. Wang, S. G. Louie, M. F. Crommie, Giant bandgap renormalization and excitonic effects in a monolayer transition metal dichalcogenide semiconductor. *Nat. Mater.* **13**, 1091–1095 (2014).
25. H. Fang, H. A. Bechtel, E. Plis, M. C. Martin, S. Krishna, E. Yablonovitch, A. Javey, Quantum of optical absorption in two-dimensional semiconductors. *Proc. Natl. Acad. Sci. U.S.A.* **110**, 11688–11691 (2013).
26. K. F. Mak, M. Y. Sfeir, Y. Wu, C. H. Lui, J. A. Misewich, T. F. Heinz, Measurement of the optical conductivity of graphene. *Phys. Rev. Lett.* **101**, 196405 (2008).
27. T. Low, A. S. Rodin, A. Carvalho, Y. Jiang, H. Wang, F. Xia, A. H. Castro Neto, Tunable optical properties of multilayer black phosphorus thin films. *Phys. Rev. B* **90**, 075434 (2014).
28. C. Lin, R. Grassi, T. Low, A. S. Helmy, Multilayer black phosphorus as a versatile mid-infrared electro-optic material. *Nano Lett.* **16**, 1683–1689 (2016).
29. F. Wang, G. Dukovic, L. E. Brus, T. F. Heinz, The optical resonances in carbon nanotubes arise from excitons. *Science* **308**, 838–841 (2005).
30. F. Wang, D. J. Cho, B. Kessler, J. Deslippe, P. J. Schuck, S. G. Louie, A. Zettl, T. F. Heinz, Y. R. Shen, Observation of excitons in one-dimensional metallic single-walled carbon nanotubes. *Phys. Rev. Lett.* **99**, 227401 (2007).
31. J. Camassel, P. Merle, H. Mathieu, A. Chevy, Excitonic absorption edge of indium selenide. *Phys. Rev. B* **17**, 4718–4725 (1978).
32. A. N. Rudenko, M. I. Katsnelson, Quasiparticle band structure and tight-binding model for single- and bilayer black phosphorus. *Phys. Rev. B* **89**, 201408(R) (2014).
33. A. Chaves, M. Z. Mayers, F. M. Peeters, D. R. Reichman, Theoretical investigation of electron-hole complexes in anisotropic two-dimensional materials. *Phys. Rev. B* **93**, 115314 (2016).

Downloaded from http://advances.sciencemag.org/ on November 19, 2018

34. A. Morita, Semiconducting black phosphorus. *Appl. Phys. A* **39**, 227–242 (1986).
35. A. Castellanos-Gomez, L. Vicarelli, E. Prada, J. O. Island, K. L. Narasimha-Acharya, S. I. Blanter, D. J. Groenendijk, M. Buscema, G. A. Steele, J. V. Alvarez, H. W. Zandbergen, J. J. Palacios, H. S. J. van der Zant, Isolation and characterization of few-layer black phosphorus. *2D Mater.* **1**, 025001 (2014).
36. T. Olsen, S. Latini, F. Rasmussen, K. S. Thygesen, Simple screened hydrogen model of excitons in two-dimensional materials. *Phys. Rev. Lett.* **116**, 056401 (2016).
37. H. Asahina, A. Morita, Band structure and optical properties of black phosphorus. *J. Phys. C* **17**, 1839–1852 (1984).
38. T. Low, R. Roldán, H. Wang, F. Xia, P. Avouris, L. M. Moreno, F. Guinea, Plasmons and screening in monolayer and multilayer black phosphorus. *Phys. Rev. Lett.* **113**, 106802 (2014).
39. V. Tran, R. Fei, L. Yang, Quasiparticle energies, excitons, and optical spectra of few-layer black phosphorus. *2D Mater.* **2**, 044014 (2015).
40. L. V. Keldysh, Coulomb interaction in thin semiconductor and semimetal films. *JETP Lett.* **29**, 658 (1979).
41. S. C. B. Mannsfeld, B. C.-K. Tee, R. M. Stoltenberg, C. V. H.-H. Chen, S. Barman, B. V. O. Muir, A. N. Sokolov, C. Reese, Z. Bao, Highly sensitive flexible pressure sensors with microstructured rubber dielectric layers. *Nat. Mater.* **9**, 859–864 (2010).
42. N. J. Farcich, J. Salonen, P. M. Asbeck, Single-length method used to determine the dielectric constant of polydimethylsiloxane. *IEEE Trans. Microw. Theory Tech.* **56**, 2963–2971 (2008).
43. P. Li, I. Appelbaum, Electrons and holes in phosphorene. *Phys. Rev. B* **90**, 115439 (2014).

Acknowledgments
Funding: H.Y. is grateful to the financial support from the National Young 1000 Talents Plan, the National Key Research and Development Program of China (grant numbers 2016YFA0203900 and 2017YFA0303504), and the Oriental Scholar Program from Shanghai Municipal Education Commission. G.Z. acknowledges financial support from China Postdoctoral Science Foundation (grant number 2016M601489). A.C. acknowledges financial support from CNPq, through the PQ and PRONEX/FUNCAP programs. Part of the experimental work was carried out in Fudan Nanofabrication Lab. **Author contributions:** H.Y. initiated the project and conceived the experiments. G.Z. prepared the samples and performed the measurements with assistance from S.H., F.W., and Q.X. T.L. and A.C. provided modeling and theoretical support. H.Y., G.Z., T.L., and A.C. performed data analysis. H.Y. and G.Z. co-wrote the manuscript with inputs from T.L. and A.C. H.Y. supervised the whole project. All authors commented on the manuscript. **Competing interests:** The authors declare that they have no competing interests. **Data and materials availability:** All data needed to evaluate the conclusions in the paper are present in the paper and/or the Supplementary Materials. Additional data related to this paper may be requested from the authors.

Submitted 19 September 2017
Accepted 6 February 2018
Published 16 March 2018
10.1126/sciadv.aap9977

Citation: G. Zhang, A. Chaves, S. Huang, F. Wang, Q. Xing, T. Low, H. Yan, Determination of layer-dependent exciton binding energies in few-layer black phosphorus. *Sci. Adv.* **4**, eaap9977 (2018).

Downloaded from http://advances.sciencemag.org/ on November 19, 2018

Science Advances

Determination of layer-dependent exciton binding energies in few-layer black phosphorus

Guowei Zhang, Andrey Chaves, Shenyang Huang, Fanjie Wang, Qiaoxia Xing, Tony Low and Hugen Yan

Sci Adv **4** (3), eaap9977.
DOI: 10.1126/sciadv.aap9977

ARTICLE TOOLS http://advances.sciencemag.org/content/4/3/eaap9977

SUPPLEMENTARY MATERIALS http://advances.sciencemag.org/content/suppl/2018/03/12/4.3.eaap9977.DC1

REFERENCES This article cites 43 articles, 2 of which you can access for free
http://advances.sciencemag.org/content/4/3/eaap9977#BIBL

PERMISSIONS http://www.sciencemag.org/help/reprints-and-permissions

Use of this article is subject to the Terms of Service

Science Advances (ISSN 2375-2548) is published by the American Association for the Advancement of Science, 1200 New York Avenue NW, Washington, DC 20005. 2017 © The Authors, some rights reserved; exclusive licensee American Association for the Advancement of Science. No claim to original U.S. Government Works. The title *Science Advances* is a registered trademark of AAAS.

Downloaded from http://advances.sciencemag.org/ on November 19, 2018